TASK QUARTERLY 14 No 3, 257–269

NUMERICAL MODELLING OF THERMOACOUSTIC PHENOMENON AS CONTRIBUTION TO THERMOACOUSTIC ENGINE MODEL

LESZEK REMIORZ, SŁAWOMIR DYKAS
AND SEBASTIAN RULIK

Institute of Power Engineering and Turbomachinery,
Silesian University of Technology,
Konarskiego 18, 44-100 Gliwice, Poland
leszek.remiorz@polsl.pl

(Received 8 June 2010; revised manuscript received 28 August 2010)

Abstract: The presented paper shows our first step into the numerical modelling of the thermoacoustic phenomenon. The thermoacoustic effect has a great application potential, for instance, in thermoacoustic engines or thermoacoustic mixture separation. These two applications are in the centre of our interest. The modelling of thermoacoustic effects consists in a solution of transport equations, mass, momentum and energy, to identify the influence of heat transfer on the sonic oscillation and vice versa. The numerical modelling of such sensitive and sophisticated phenomena requires a high quality numerical tool. The commercial CFD code ANSYS CFX 12 was chosen as the numerical tool. This investigation will be supported by using the finite time thermodynamic theory.

At the beginning preliminary numerical tests were performed in order to validate the numerical methods and the boundary conditions implemented in CFX. The numerical calculations of the Rijke tube were carried out and the results were validated against analytical relations.

Keywords: thermoacoustic engine, Rijke tube

1. Introduction

Nowadays, the intensive search for low emissive and highly efficient power technologies is still underway. The power, aircraft and automotive industries are faced with stricter emission norms. The conventional energy sources are not always able to meet increasing numbers of requirements connected with a reduction of the harmful impact on the environment, availability, maintenance costs and with many other parameters. It is especially visible in the so called "small" power systems. Therefore, the development of new technologies based on the

thermoacoustic phenomenon, new devices working on the basis of the Stirling cycle, are very interesting and promising.

The research on the numerical modelling of acoustic waves generation and propagation seems to be worth striving for. For the time being we have mainly focused our attention on the acoustic waves generation in an aerodynamic way [1] and their propagation [2] in both the near and far acoustic fields. The acoustic fluctuations in the flow field occur mainly as a result of the turbulence effects caused by the flow or heat conduction at the wall.

Numerical modelling of the acoustic waves propagation induced in an aerodynamic way is well known and has been in the centre of interest of many researchers for over 20 years. The forced limitations regarding the emission of environmental as well as machinery noise, the fast development of the CFD techniques and computational capability have accelerated the research on the Computational Aero-Acoustics (CAA) and Thermo-Acoustics (CTA) rapidly.

A thermoacoustic phenomenon exists widely in the power and automotive industries as an effect. It is responsible for an instability in gas turbine combustors or pulse combustors. It can be used also in coal combustors to limit the emission of small ash particles (smaller that 5 microns), the acoustic energy helps these particles coalesce into a bigger size, more convenient for conventional ash removing methods. The possibilities of the acoustic waves application are very wide in fulfilling stricter emission standards, however, they are unfortunately underestimated. We hope that our research will allow a new and fresh insight into the problems connected with aero-and thermoacoustic waves.

2. Some theory

Thermoacoustics refers to the generation of acoustic waves due to the heat transfer or inversely, to the induction of the heat gradient sonically. These phenomena have been known for many years. A thermoacoustic phenomenon was firstly described by Rayleigh over 100 years ago [3]. The theoretical background was provided in the 80s and 90s of the last century by Weatley [4] and Swift [5] from the Los Alamos National Laboratory (USA). The nature of this phenomena consists in the spontaneous acoustic waves excitation in the specially formed channels due to heat addition. This phenomenon is reversible, i.e. that the propagation of the acoustic waves in the channel under special conditions may trigger off a heat flow.

Thermoacoustic phenomena classified as thermally induced spontaneous oscillations were investigated in a resonance tube by Rijke at the end of the 19^{th} century. The Rijke tube is a convenient system for studying thermoacoustic instabilities in devices with a mean flow with forced velocity or free convection.

3. Rijke tube

The sound production in a Rijke tube is a classical example of a thermoacoustic phenomenon. It was discovered by Rijke around 1850. A classical Rijke

resonance tube is an open pipe of length L, with two open ends (Figure 1), positioned vertically. The flow in the tube is induced by free convection. In the case of a horizontal position of the tube the flow has to be forced, *e.g.* by a blower. The travelling sound waves which are produced inside the tube move in opposite directions. When the waves reach both ends of the tube, some part of them reflect from the surrounding air. Afterward, they interact and a standing wave is formed inside the tube as a result.

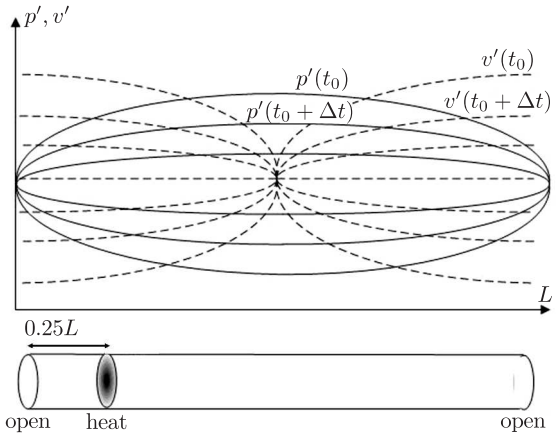

Figure 1. Rijke resonance tube

Figure 1 presents the distribution of the acoustic pressure and acoustic velocity in a function of the Rijke Tube length. In this case local pressure p and local velocity v are a sum of mean part p_{mean}, v_{mean} and acoustic part p', v'. The acoustic pressure and velocity are in an opposite phase. To produce and sustain the acoustic waves the heat has to be transferred to the air at the moment of the greatest compression and taken at the moment of the greatest expansion [3]. The heat transfer in case of the Rijke Tube is not constant and can be divided into mean part q_{mean} and fluctuating part q'. It means that the heat transfer varies with the change of the acoustic pressure and velocity due to changes in the temperature difference between the air and the heating element. The acoustic waves are driven only in case when the heat transfer fluctuating part q' and acoustic pressure p' are in phase. It happens only for the lower part of the Rijke Tube where the heating element is located. The best position for the heating element is located at a quarter of a tube length of $0.25L$.The frequency of the sound waves generated by the Rijke Tube depends only on the tube length.

4. Thermoacoustic cycle

The interaction between heat and sound can be applied in various technologies without any adverse environmental impact. Unfortunately, the thermoacoustic systems developed to date have low power density and low thermal efficiency. Therefore, their applications should be associated with the use of waste heat. It

has been found that the phasing of acoustic velocity and pressure in a traveling acoustic wave is similar to that of the Stirling cycle [6, 7] (Figure 2). In the case of a standing wave the pressure and velocity are not in phase. It will be presented in our further calculation results. Both traveling wave and standing wave engines have been under investigation of many researchers.

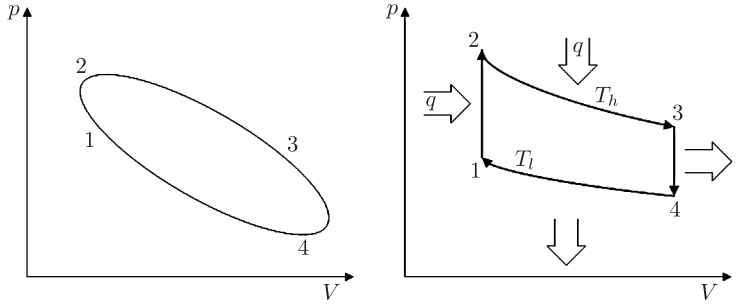

Figure 2. Stirling cycle

Our numerical studies will be conducted in order to understand thoroughly and to model correctly the energy transport and conversion in a thermoacoustic engine, in a device without moving parts.

5. Numerical simulation and results

The application of the CFD techniques for modeling of the thermoacoustic phenomena is now possible and it is necessary to include issues important for a thermoacoustic engine design (see *e.g.* [8] or [9]).

The first numerical simulations were focused on the validation of the Rijke oscillation modeling. It has been already mentioned that the wavelength of the standing acoustic wave depends on the tube length only, and it should be easily to validate. The open-open Rijke tube was selected for the presented CFD studies. The geometry of the tube presented in Figure 3 was chosen for calculations. However, the numerical domain was limited to one segment of the convector only. The selected part consisted of one full heating element. It allowed speeding up the calculation process, which is very time consuming for a transient simulation. The real geometry consisted of several segments of a convector, what has been shown in the discussion of the results further in the paper. The pure 2D simulation was performed with the use of commercial software Ansys-CFX12. It means that only one element of a numerical grid was used in the spanwise direction.

Outer numerical domains were added at the tube inlet and outlet. Proper modeling of the boundary conditions at the tube ends is crucial in the case of an open-open resonance tube. The part of the acoustic wave excited inside the tube leaves the tube and the rest reflects creating a standing wave inside the tube. Our previous calculations had shown that no boundary condition implemented in CFX could model this effect properly. Due to this fact additional surrounding domains were modeled. It allowed specifying the boundary conditions relatively far from

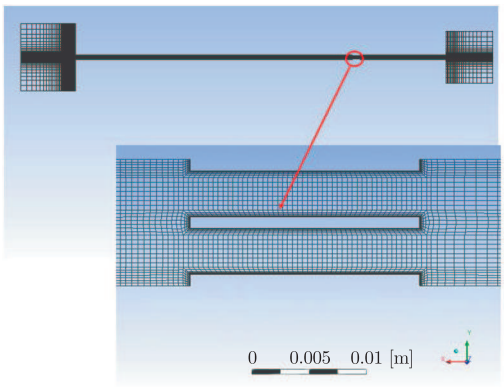

Figure 3. Scheme of geometry and numerical mesh of Rijke tube

the Rijke tube inlet and outlet. Additionally, it allowed tracing the acoustic waves outside the tube and investigating what would happen when the waves left the Rijke tube.

The length of the tube was $L = 1\,\mathrm{m}$, what gives the frequencies of oscillations of about $f = c/\lambda = 340/2 = 170\,\mathrm{Hz}$. The heater element (convector) was located at a distance of $L/4 = 0.25\,\mathrm{m}$. The plates of the convector were 20 mm long and 1 mm thick. The distance between the plates was 4 mm.

The structural mesh was prepared for the purpose of numerical studies. The mesh consisted of 60 000 nodes. The O-grid mesh was used around the heating elements (Figure 3). The application of O-grid mesh type allowed using larger elements in the upstream and downstream direction and decreasing the overall number of nodes. The upstream part of the device was meshed with 150 elements in direction x and the downstream part which was 3 times longer was meshed with 500 elements. Grid stretching was applied in both outer domains in order to use the larger mesh elements and decrease the overall number of nodes. The main flow resulting mainly from free convection is shown from right to left in Figure 3, but in the reality the tube was placed vertically. Buoyancy direction x was assumed in the numerical studies. The open boundary conditions with the static relative pressure of 0 Pa and temperature of 300 K were assumed. The specified boundary conditions allowed imitating the real work environment of the Rijke tube. In this case it was only the free convection that was responsible for the flow inside the tube.

The symmetry boundary condition was applied for both sides of the calculation domain. The symmetry was also used for the upper and lower surfaces of the domain and for the outer cavities. It was only for the heating element that the wall boundary condition was set up with the wall temperature equal to 1200 K.The high temperature makes it possible to decrease the heating element size keeping the input heat flux constant. However, smaller heating elements decrease the number of elements of the numerical mesh. In Figure 4 the scheme of the assumed boundary conditions is presented.

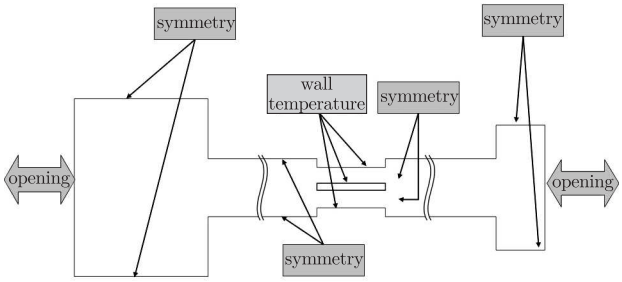

Figure 4. Boundary conditions assumed in modeling

The specified time step was set to $\Delta t = 5 \cdot 10^{-5}$ s. The influence of the time step for the results was also a subject of our investigation. Too large a time step affects the constant decrease in the acoustic waves amplitude. Nevertheless, shorter time steps yield results similar to the time step selected in the calculations. The specified time step corresponds to 100 iterations per one period and seems to be a good compromise between the accuracy and the calculation time. The maximum number of coefficient loops per one iteration was set up to 10. Usually, about 5 loops were necessary to obtain the established convergence criteria. The pressure and velocity oscillations are strongly connected with temperature variations. Due to this fact it is important to obtain a proper temperature distribution inside the tube. However, for this purpose a long period of time is necessary. Usually the process takes a few seconds. It means that for the specified time step a large number of iterations have to be carried out, what is time consuming. To speed up the process, the steady state solution is calculated first. This solution may be obtained in two ways. The first one is a separate steady state solution and the second one are transient calculations with very large time steps. To this end the time step size in the iteration number function was specified. It allows gradually increasing the time step size. The maximum value is equal to 0.01 s. Usually, about 2.5 seconds are necessary to obtain a steady state solution. After the steady state solution had been obtained the time step size was decreased and the proper calculation process started. The initial pressure disturbance was introduced to get the oscillations. Without that the device would stay in a steady state. Even a very small perturbation may disturb the equilibrium state. In the presented case the pressure impulse of 30 Pa was set up. The amplitude and time of the pulse are also important. If the pulse is to weak the device may return to the equilibrium state and in case of too strong a pulse, the device oscillations may be distorted by the initial pressure pulse. The proper choice of the initial pulse gives pressure oscillations which have a similar amplitude during the first few thousand iterations and afterward the amplitude starts increasing gradually.

Figure 5 and Figure 6 present the velocity and temperature contours obtained in steady state calculations. The inlet velocity was about 1.0 m/s and the velocity reached about 1.6 m/s after the passage through the heating

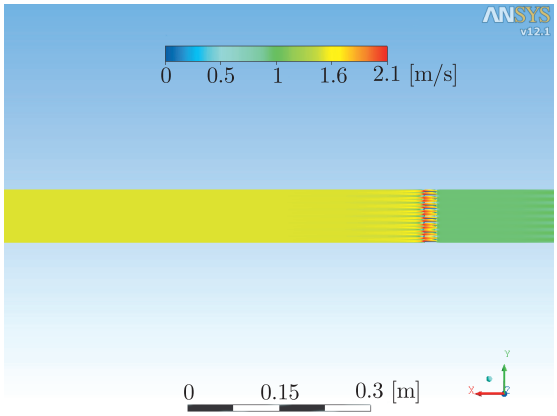

Figure 5. Velocity contour for steady state solution

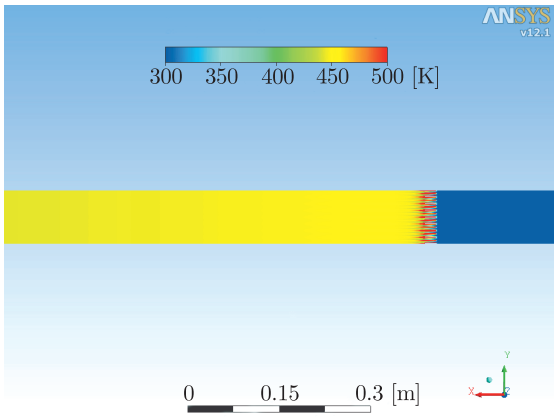

Figure 6. Temperature contour for steady state solution

elements. The temperature varied from 300 K to about 450 K in the downstream direction.

All the presented contour plots are obtained by copying the results obtained only for a single heating element. A total of 15 elements are presented for better visualization of the results. However, the real thermoacoustic engine may consists of a few hundred ore even a few thousand heating elements.

During the calculation process the values of the main parameters were monitored in 5 different locations. The first point was located in the inlet cross-section. Points 2 and 3 were located in front of and behind the heating element. Point 4 was 0.05 m behind the outlet cross-section. Monitor point 5 was in the outlet outer cavity at a distance of 0.07 m from the outlet cross-section. Figure 7 presents the location of selected monitor points.

The initial process which illustrates the disturbance introduced into the tube and pressure oscillations excitations are presented in Figure 8. The pressure

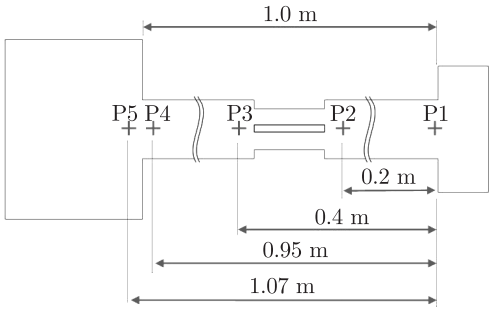

Figure 7. Location of monitor points

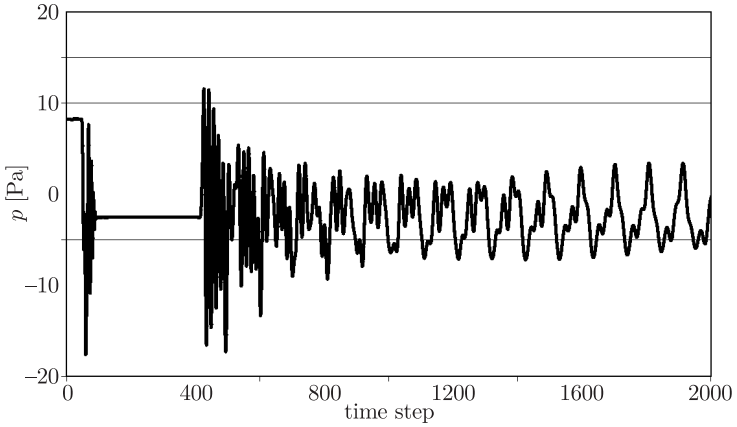

Figure 8. Initial pulse and pressure oscillations excitations in function of time step

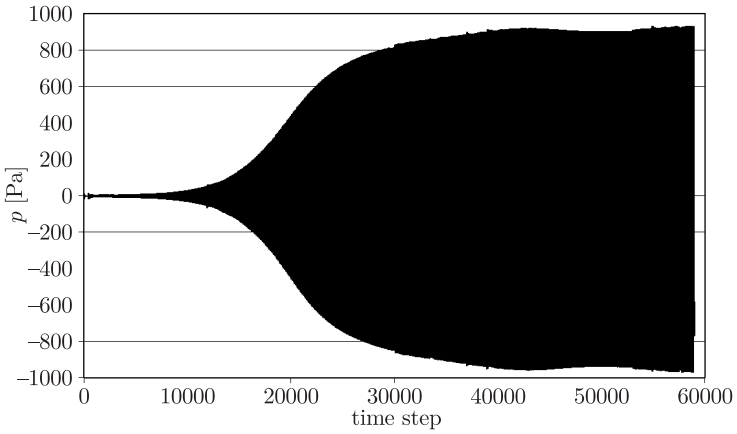

Figure 9. Pressure oscillations in function of time step

distribution in a function of time steps is gathered for monitor point 3 located at a distance of 0.3 m from the inlet and about 0.05 m from the heating elements.

In this case the first 400 iterations were calculated with very large time steps. It allowed increasing the heating process speed and obtaining a steady state

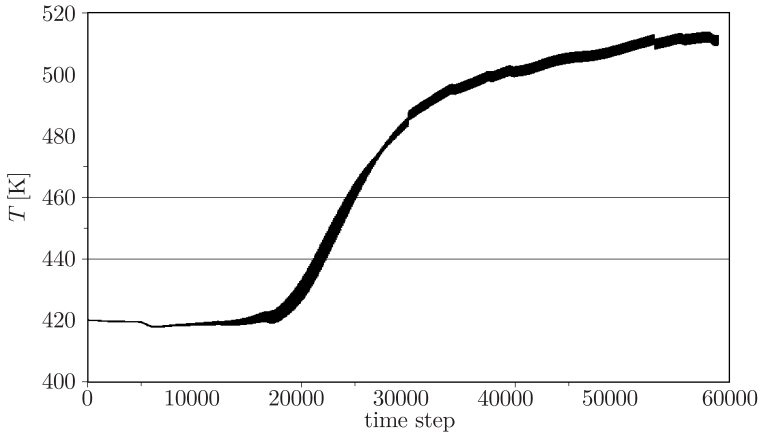

Figure 10. Temperature oscillations in function of time step

solution (Figures 5 and 6). This process took about 2.5 seconds. Afterward, the initial disturbance was introduced and the pressure started oscillating. The initial pulse amplitude was lower than the selected 30 Pa due to the distance between the domain boundary and the Rijke tube inlet cross-section. Additionally, poor quality mesh was applied for the inlet outer cavity what increased the numerical dissipation of the pressure pulse.

Figure 9 presents the pressure oscillations in a function of time step during the whole calculation process. The reference pressure in this case is equal to atmospheric pressure. The 60 000 iterations were performed during the simulation what corresponds to the total time of simulations of 5.5 s.

The obtained frequency of the pressure oscillations was equal to about $f = 1/T = 200$ Hz what corresponds to a 18 % error in comparison with the theoretical value of 170 Hz. The proper frequency of the acoustic waves was achieved after about 5 000 time steps. However, about 40 000 time steps were necessary to obtain the limit cycle of the pressure oscillations. The temperature fluctuations were also monitored during the simulation. The temperature value for monitor point 3 (Figure 10) rose from about 420 K, what corresponded to the steady state solutions, to about 510 K at 60 000 iterations.

However, the differences in temperature level do not strongly interact with the pressure oscillations. It must be emphasized that a crucial element is the temperature amplitude and not the temperature level.

Figure 11 and Figure 12 present the pressure fluctuations in a function of time step for different monitor points locations. The maximum amplitude was reached for monitor point 3 located just behind the convector. The amplitude in front of the convector was equal to about 700 Pa. The amplitude near the outlet region (Monitor point 4) was equal to 200 Pa. The values of the mean pressure and velocity are similar to those obtained in steady state calculations.

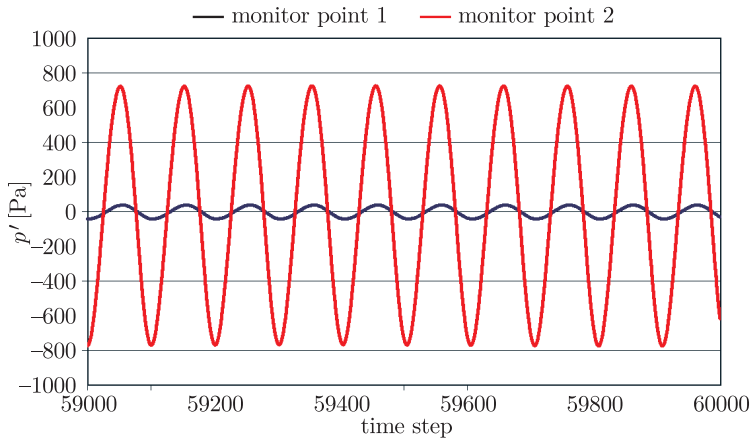

Figure 11. Pressure fluctuations for monitor points 1, 2

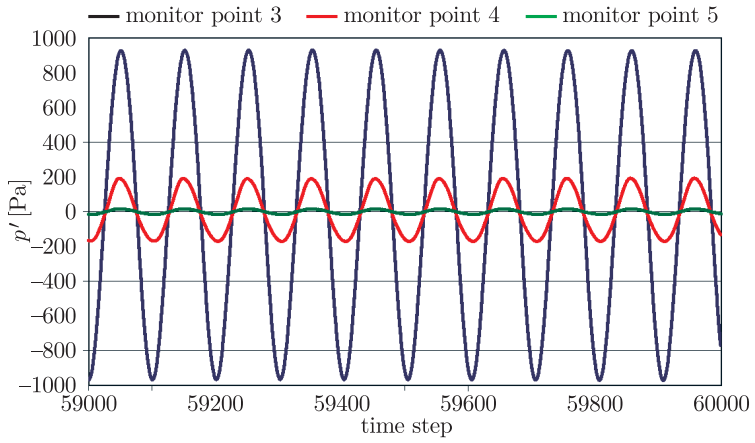

Figure 12. Pressure fluctuations for monitor points 3, 4, 5

A comparison between two points located inside and outside the tube (Monitor point 4 and 5) at a distance of 0.07 m was also made (Figure 12). The pressure amplitude outside the tube is an order of magnitude lower.

The Fast Fourier Transformation (FFT) was also performed for these two points and the results are presented in Figure 13. The maximum sound pressure level (SPL) was equal to 135 dB for monitor point 4 and outside the tube (Monitor point 5) the SPL was equal to 115 dB. The maximum SPL corresponding to the fundamental frequency was equal to 200 Hz.

The constant compression and expansion of the gas particles causes the temperature of the gas to change periodically. It means that the temperature difference between the heating element and the surrounding gas changes and has significant influence on the predicted heat flux. The oscillations of the heat flux delivered to the gas inside the Rijke tube are presented in Figure 13. The amplitude is equal to about 4 000 W/m^2.

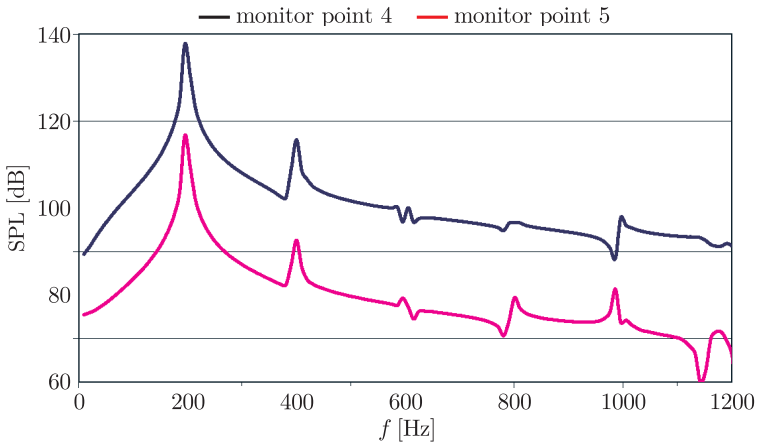

Figure 13. FFT for monitor point 4 and 5

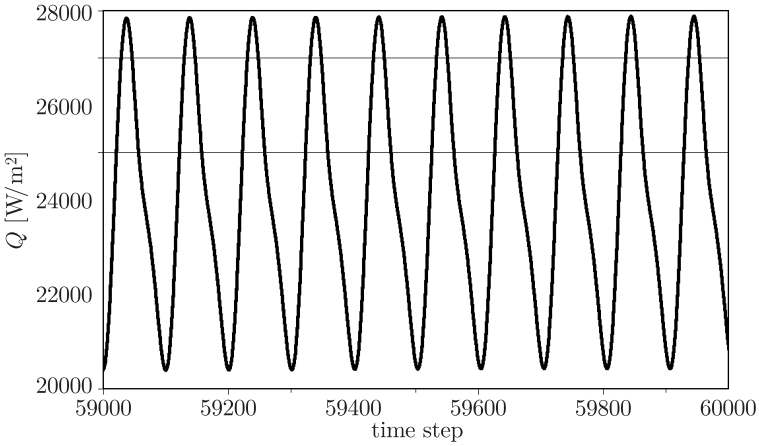

Figure 14. Heat flux fluctuations

Figure 14 presents one full period of the pressure wave inside the Rijke tube.

The left column in Figure 15 shows snapshots of the pressure distribution and the right column presents the corresponding charts of pressure distribution along the tube length. It is well visible that fixed nodes of the pressure wave appear at both ends of the tube. It proves the standing wave form inside the Rijke tube.

6. Conclusions

It is the validation tests that decide whether the assumed numerical tool and the available methods are efficient or not. The good quality of the assumed method for modeling the acoustic oscillation frequencies was proved for assessing thermoacoustic phenomena. The generated standing acoustic wave in a resonance tube had a correct position of the nodes and antinodes. Unfortunately, it was

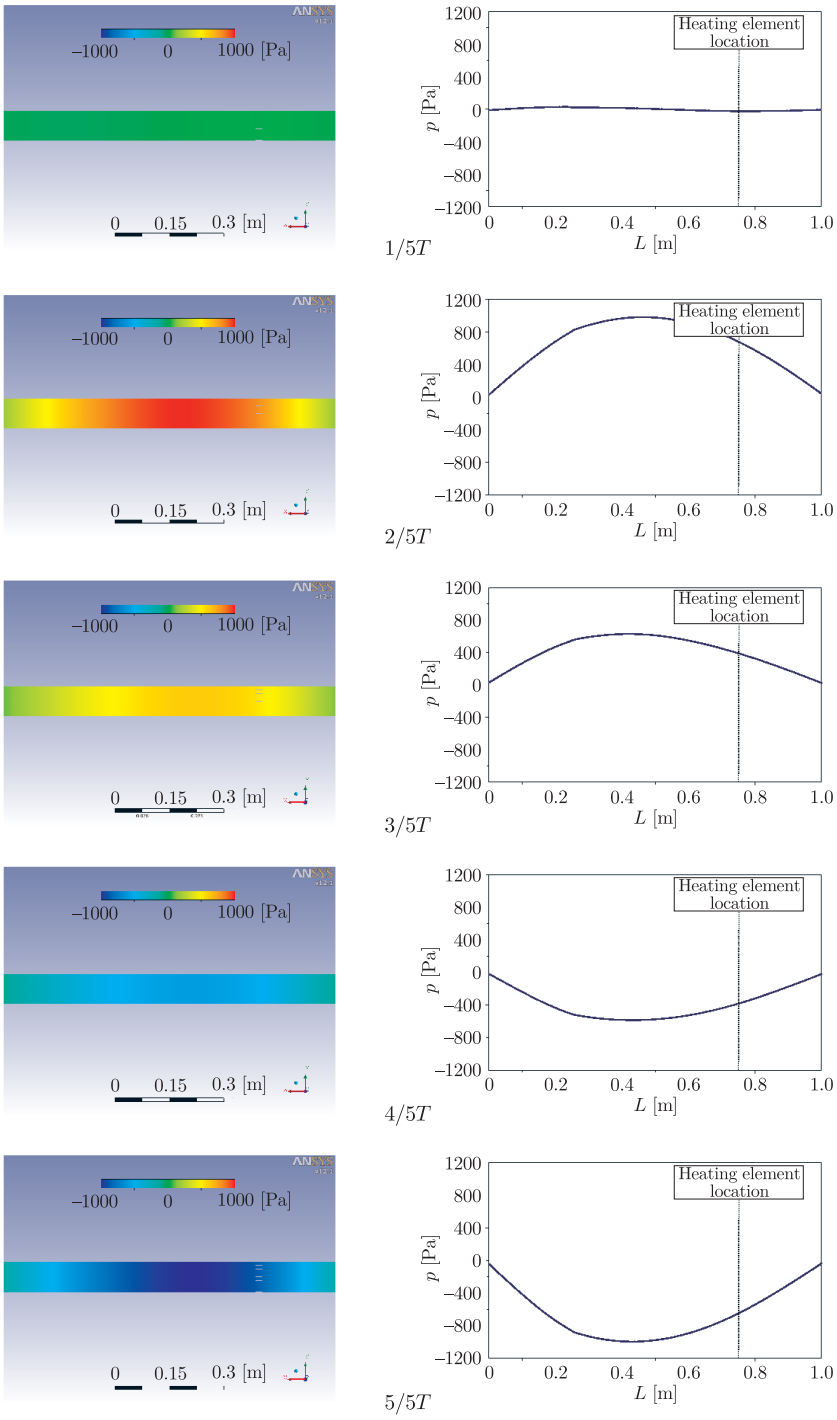

Figure 15. Snapshots of one full period of acoustic wave inside the tube

very difficult to find a test to validate the correctness of the acoustic wave amplitude.

The future research will be focused on the search for a relation between the heat flux and the acoustic wave amplitude, what is crucial for correct modeling of a thermoacoustic engine or for the mixture separation.

Acknowledgements

The investigations presented in this paper have been conducted within the framework of research project no NN512316938 of Polish Ministry of Science and Higher Education.

References

[1] Dykas S, Wróblewski W and Chmielniak T 2006 *Inżynieria Chemiczna i Procesowa* **27** (3/1) 685
[2] Dykas S, Wróblewski W, Rulik S and Chmielniak T 2010 *Archives of Acoustics* **35** (1) 35
[3] Lord Rayleigh 1945 *The Theory of Sound*, Vol. II, Dover, New York
[4] Wheatley J, Hofler T, Swift G W and Migliori A 1985 *Am. J. Phys.* **53** (2) 147
[5] Swift G W 1988 *J. Acoust. Soc. Am.* **84** (4) 1148
[6] Ceperley P H 1979 *J. Acoust. Soc. Am.* **66** 1508
[7] Ceperley P H 1982 *J. Acoust. Soc. Am* **77** 1239
[8] Hantschk C C and Vortmeyer D 1999 *J. Sound and Vibration* **277** (3) 511
[9] Zink F, Vipperman J and Schaefer L 2010 *Int. Commun. in Heat and Mass Transfer* **37** 226